MECOM99
Mendoza
6-10 de septiembre de 1999

A TIME-DOMAIN SIMULATION FOR EVALUATING SMART WING CONCEPTS

Benjamin D. Hall[a], Sergio Preidikman[b], Dean T. Mook[a], and Ali H. Nayfeh[a]

[a]Department of Engineering Science and Mechanics
Virginia Polytechnic Institute and State University
Blacksburg, VA 24061-0219, USA

[b]Facultad de Ingeniería
Universidad Nacional de Río Cuarto
Ruta Nacional 36 Km 601
(5800) Río Cuarto, Provincia de Córdoba, Argentina

RESUMEN

En este trabajo se presenta el desarrollo e implementación de una simulación numérica que permite evaluar métodos para controlar la respuesta de un ala elástica en flujo inestacionario o estacionario. La simulación consiste de cinco partes: un modelo para la estructura del ala, un modelo para el flujo de aire, un modelo para el sistema de control, un método que permita combinar los modelos anteriormente citados, y un esquema numérico para integrar, interactívamente y simultáneamente, en el dominio del tiempo las ecuaciones de movimiento. El flujo de aire, la estructura del ala, y el sistema de control son considerados como elementos componentes de un único sistema dinámico. El método propuesto es modular; esto permite realizar modificaciones a cada uno de los subsistemas sin modificar la estructura global de la simulación. La técnica descripta en este trabajo no esta restringida al análisis de movimientos periódicos o geometrías simples. Como ejemplo de aplicación, se investiga el control activo del ala de un avión de gran autonomía y diseñado para volar a gran altitud. Se consideran condiciones de vuelo típicas que incluyen ráfagas. La estructura del ala es modeladada como una viga de Euler-Bernoulli en voladizo. El modelo estructural es lineal e incluye acoplamiento dinámico entre flexión y torsión. Las ecuaciones que describen al modelo estructural son discretizadas mediante el uso del método de elemento finitos. Para modelar la aerodinámica se utiliza nuestra versión del método general de red de vórtices discretos (Vortex-Lattice Method). Este modelo aerodinámico es inherentemente no lineal, puede ser usado para simular maniobras estacionarias y/o inestacionarias en régimen subsónico, y tiene en cuenta la historia del movimiento. Para disminuir la respuesta en "flutter" y a ráfagas, se utiliza una ley de control basada en retroalimentación. El actuador se supone distribuido a lo largo del ala. Las simulaciones numéricas muestran que el "flutter" es totalmente suprimido, sin embargo, los picos generados por ráfagas son marginalmente reducidos.

ABSTRACT

A numerical simulation for predicting and evaluating methods to control the response of an elastic wing in a steady or an unsteady airstream is discussed. The simulation consists of five parts: a model of the structure, a model of the flowfield, a model of the control system, a method for combining the models, and a numerical scheme to integrate all of the governing equations interactively and simultaneously in the time domain. The approach considers the air, the deforming wing, and the controller as elements of a single dynamical system. The method is modular, allowing independent modifications to the aerodynamic, structural, and control subsystems and it is not restricted to periodic motions or simple geometries. As a demonstration of the technique and its capabilities, we investigate the active control of a High Altitude, Long Endurance (HALE) aircraft wing in typical flight conditions, including gusts. The wing is modeled structurally as a linear Euler-Bernoulli beam that includes dynamic coupling between the bending and torsional oscillations. It is discretized via finite-elements. Our version of the general nonlinear unsteady vortex-lattice method, which is capable of simulating arbitrary subsonic maneuvers of the wing and accounts for the history of the motion, is employed to model the aerodynamics. Feedback control via a distributed actuator is used for flutter and gust-load alleviation. In the simulations, flutter is readily suppressed, but presently, peak gust loads are only marginally reduced.

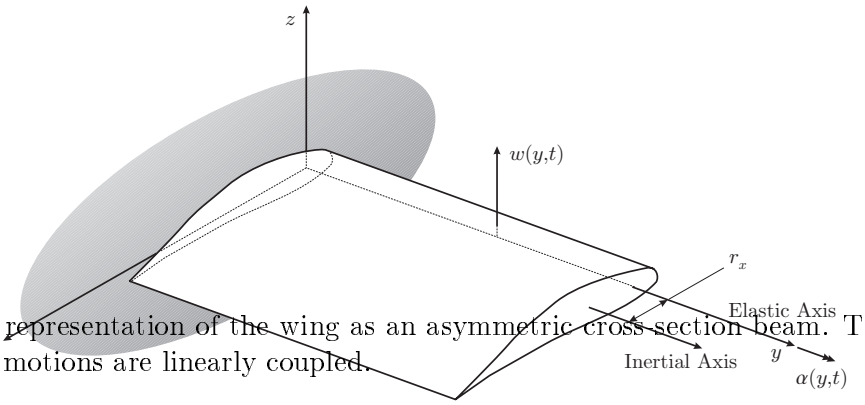

Figure 1: Structural representation of the wing as an asymmetric cross-section beam. The bending $w(y,t)$ and torsional $\alpha(y,t)$ motions are linearly coupled.

INTRODUCTION

In this paper, we describe, by means of an example, a time-domain simulation that is an ideal tool to evaluate smart-wing concepts, where the interplay of structural motions, aerodynamic forces, and control forces is of great importance. We consider a typical High Altitude, Long Endurance (HALE) aircraft wing that has been modified to include sensors and an integrated actuator, which can apply a uniformly distributed torque along the span of the wing. Such a wing is an example of what is often termed a "smart wing."

There are five components of the simulation tool: a model of the structure, a model of the flowfield, a model of the control system, a method for combining the models, and a means of integrating all of the governing equations interactively and simultaneously in the time domain. We will briefly describe each of the five components that we use for the modeling of this prototypical smart HALE aircraft wing and then present some results of the simulations.

In related work, Luton and Mook[1] developed a similar numerical simulation using ailerons to control the flutter response of a high-aspect-ratio wing. Preidikman and Mook[2] have also implemented a similar technique to demonstrate the active control of the wind-excited vibrations of a suspension bridge via a small, lightweight wing attached below the roadbed. Additionally, Preidikman[3] and Preidikman and Mook[4] have used the same simulation tool used here to predict the aeroelastic response of a business jet. Currently, parallel efforts are progressing to study the effects of aeroelastic interference among the wing, pylon, and store of an F16,[5] the effects of aeroelastic interference in windmills, and the hydroelastic response of ships. Recently, Tang, Dowell, and Hall[6] performed a somewhat comparable aeroelastic analysis of a plate including von Karman nonlinearities in the model and using a reduced-order, linear vortex-lattice method.

THE STRUCTURAL MODEL

HALE aircraft typically have rather flexible, high-aspect-ratio wings, and we model the wing structurally as a cantilevered Euler-Bernoulli beam that has linear, dynamic coupling between the bending and twisting motions. Such a beam is shown in Figure 1, where we see that the centroidal or inertial axis (i.e., the locus of mass centers of the beam cross-sections) and the elastic axis (i.e., the locus of shear centers of the beam cross-sections) are offset by a distance r_x in the x-direction; consequently, the bending and twisting motions are coupled through the inertia terms. For the present, we assume that the wing is inextensional and bends only in the z-direction.

For beams with nonsymmetric cross-sections experiencing torsion and bending in one plane only, the governing equations have been derived by Timoshenko,[7] Bisplinghoff, Holt, and Ashley,[8] and Fung[9] using the

Newtonian approach and by Rao[10] using Hamilton's principal. They are

$$\left[EI(y)w''(y,t)\right]'' + \mu(y)\ddot{w}(y,t) - \mu(y)r_x(y)\ddot{\alpha}(y,t) = Q_w(w,\dot{w},\ddot{w},\alpha,\dot{\alpha},\ddot{\alpha},y,t,history) \tag{1}$$

$$-\left[GJ(y)\alpha'(y,t)\right]' + I_p(y)\ddot{\alpha}(y,t) - \mu(y)r_x(y)\ddot{w}(y,t) = Q_\alpha(w,\dot{w},\ddot{w},\alpha,\dot{\alpha},\ddot{\alpha},y,t,history) \tag{2}$$

where primes denote derivatives with respect to the spanwise coordinate y and dots are time derivatives. The physical properties are the bending stiffness $EI(y)$, the torsional rigidity $GJ(y)$, the mass per unit length $\mu(y)$, and the polar moment of inertia $I_p(y)$ of the beam; $r_x(y)$ is the separation of the mass (inertial) and elastic axes in the xy-plane. The terms $Q_w(\cdots)$ and $Q_\alpha(\cdots)$ are the generalized forces on the beam and include both the aerodynamic and control forces.

For the simulation, we will use a reduced set of the modal equations of motion. To obtain these, we employ the finite-element method and discretize the structure by expanding the motion as

$$w(y,t) = \sum_{j=1}^{2N} \eta_j(y)d_j(t) \tag{3}$$

$$\alpha(y,t) = \sum_{j=1}^{N} \Theta_j(y)e_j(t) \tag{4}$$

where N is the number of elements in the finite-element discretization. Unlike the classical Rayleigh-Ritz method, these trial functions are local functions and we use the simplest set, namely the linear finite-element approximation functions for the torsional discretization and Hermite cubic interpolation functions for the bending discretization.[11]

Without going into the details, we obtain the spatially discretized equations by substituting expansions (3) and (4) into equations (1) and (2), premultiplying the first equation by $\eta_i(y)$ and the second by $\Theta_i(y)$, and integrating over the length of the beam. The result is:

$$\tilde{M}\ddot{\mathbf{x}}(t) + \tilde{K}\mathbf{x}(t) = \mathbf{F}(\mathbf{x},\dot{\mathbf{x}},\ddot{\mathbf{x}},t,history) \tag{5}$$

which is a set of $3N$ coupled equations, N of which correspond to translational motion, $w(y,t)$, and have dimensions of force while the remaining $2N$ equations correspond to rotational motion, $\alpha(y,t)$ and $w'(y,t)$, and have dimensions of moment. Here $\mathbf{x}(t)$ is the vector of nodal displacements and rotations, $d_j(t)$ and $e_j(t)$.

The finite-element equations are uncoupled by introducing the transformation $\mathbf{x}(t) = \Phi\mathbf{y}(t)$ into equations (5), where Φ is the modal matrix defined such that the equations become

$$M\ddot{\mathbf{y}}(t) + K\mathbf{y}(t) = \Phi^T\mathbf{F}(\mathbf{y},\dot{\mathbf{y}},\ddot{\mathbf{y}},t,history) \tag{6}$$

where both M and K are diagonal matrices and $\mathbf{y}(t)$ is the dimensionless modal vector of length $3(N-1)$. Premultiplying equation (6) by M^{-1} we obtain the governing equations for the structural dynamics of the wing in terms of the finite-element modes

$$\ddot{\mathbf{y}}(t) + \bar{\Lambda}\mathbf{y}(t) = M^{-1}\Phi^T\left[\mathbf{F}_A^S(\mathbf{y},\dot{\mathbf{y}},\ddot{\mathbf{y}},t,history) + \mathbf{F}_C(t)\right] \tag{7}$$

where $\bar{\Lambda}$ is the diagonal matrix of natural frequencies squared and we have split the forcing vector into its two constituent parts, namely the control forces $\mathbf{F}_C(t)$ and the aerodynamic forces $\mathbf{F}_A^S(\mathbf{y},\dot{\mathbf{y}},\ddot{\mathbf{y}},t,history)$, which depend the modal coordinates, their time derivatives, time, and the history of the motion.

We remark that a finite-element solution is not the most efficient means of solving this particular problem and a more direct approach would have been to use a Galerkin procedure on the original governing partial-differential equations (1) and (2). We have chosen to use the finite-element method to demonstrate the versatility of the time-domain simulation tool that we have developed. All that is required for the structural module of the simulation tool are the modal matrix Φ, the modal masses M and the modal frequencies $\bar{\Lambda}$.

Examining equations (7) we recognize that they have dimensions of $\sec^{-2}$, accordingly, we nondimensionalize the system by multiplying by T_c^2 where T_c is a characteristic time that is defined in terms of the flight speed and a characteristic length of the aerodynamic wing mesh. The dimensionless governing equations are

$$\ddot{\mathbf{y}}(\tau) + \Lambda \mathbf{y}(\tau) = T_c^2 M^{-1} \Phi^T \left(\mathbf{F}_A^S + \mathbf{F}_C \right) \tag{8}$$

where dots now represent derivatives with respect to the dimensionless time $\tau = \frac{t}{T_c}$ and $\Lambda = T_c^2 \bar{\Lambda}$ is the diagonal matrix of dimensionless (or reduced) natural frequencies.

THE AERODYNAMIC MODEL

The role of the aerodynamic model is to reliably predict the unsteady loads on the wing during simulated flight conditions and that requires an accurate model of the macroscopic flowfield around the wing. We employ the general three-dimensional nonlinear unsteady vortex-lattice method for this task. It can handle arbitrary unsteady subsonic maneuvers of wings of arbitrary planform. Application of the vortex-lattice method implies a knowledge of the regions in the flowfield where vorticity is concentrated, and the method becomes unreliable when stall or vortex bursting occurs near the wing.

The vortex-lattice method has been widely used for aerodynamic simulations[12–18] and recently for fluid-structure interaction problems[1–6] as we do here. Unlike the Navier-Stokes equations, which are a highly nonlinear set of coupled partial-differential equations, the vortex-lattice method reduces the aerodynamic problem to the solving of a set of linear algebraic equations for the strength of the bound vortex sheet and a set of nonlinear ordinary-differential equations for the position of the free-vortex sheet (the wake). These equations can be solved interactively with the structural dynamic motions making the technique very appealing for use in problems involving fluid-structure interactions.

A meaningfully detailed mathematical description of the vortex-lattice method is not feasible here, so we only highlight the relevant technical aspects of the method. For more detailed explanations, see Konstadinopoulos, et al.[12] or Preidikman,[3] or the works of Belotservkoskii,[13] Belotservkoskii and Lifanov,[15] or Lewis.[16] Sarpkaya[19] gave an excellent review of numerical methods with vortices through the mid-1980s.

As a wing moves through the air, thin boundary layers, where both viscous and rotational effects are important, are created at the solid-fluid interface on its top and bottom surfaces. The wing acts as a vorticity generator, creating the vorticity in the boundary layers and then shedding that vorticity from the wing tips and trailing edge forming the wake, or free-shear layer, in the flow behind the wing. This process of vorticity generation and shedding continues as long as the wing moves.

As a precursor to applying the vortex-lattice method, we assume that all the vorticity in the flowfield is located in the boundary and free-shear layers and that those layers can be approximated as infinitely thin sheets; this is known as the infinite-Reynolds-number approximation. The boundary and free shear layers are then modeled as lattices of discrete vortex segments. On the wing lattice, we impose the no penetration condition to solve for the strength of the lattice at each time and we convect the segments of the wake lattice with the local particle velocity (thus rendering the wake a force-free surface in the flowfield). At the edges of the wing where the wake adjoins, we make the pressure difference in the airstreams along the top and bottom surfaces of the wing vanish (the unsteady Kutta condition). The aerodynamic loads are calculated by applying the general unsteady Bernoulli's equation at the control points of the aerodynamic grid shown in Figure **??**.

A sample representation of a flexible wing and the computed wake that trails it as sheets of vorticity is shown in Figure 2. Because the wake records the history of the wing motion and effects the time-dependent loading on the wing, it is often called the historian of the flow.

Gusts

In the present simulation gusts can be modeled at least two ways. First, we can give the air a perturbation

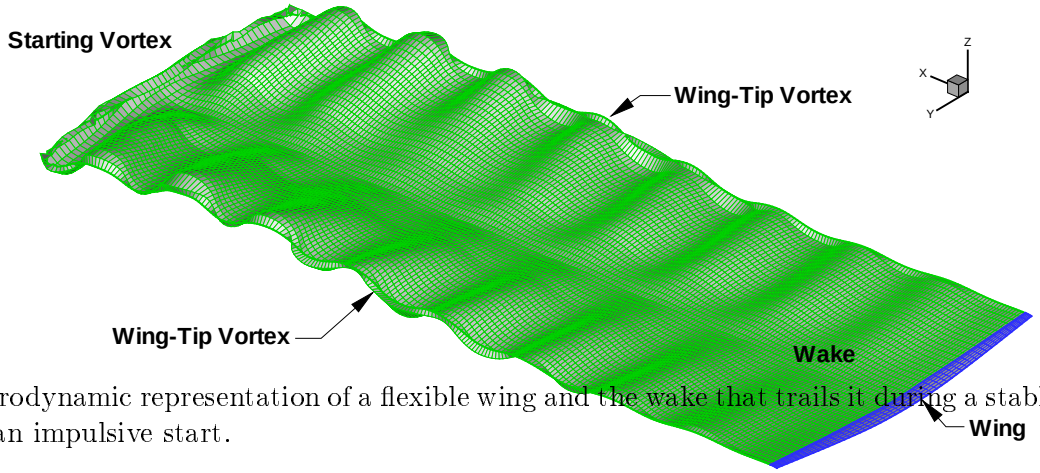

Figure 2: Aerodynamic representation of a flexible wing and the wake that trails it during a stable aeroelastic response to an impulsive start.

velocity. With this method, we can explicitly choose the frequency content, power spectral density, and amplitude of the gust. It can be spatially uniform, affecting all points in the calculation space identically at each time step, or, we can add a spatial variation. With this method, we can directly implement the normal load criteria for the design of HALE aircraft, which specifies that the vehicle be able to withstand a 50 ft/s uniform gust.[20]

The second with which we can simulate gusts is to introduce some vorticity into the flowfield in the form of discrete vortices or vortex sheets to simulate clear-air turbulence. This is a more realistic version of the atmospheric turbulence which causes gust loadings,[21] and facilitates the use of spatially nonuniform gusts, but it is more difficult to incorporate specific frequency contents into the gust signal. After the vorticity is added to the air, we "fly" the wing past it to simulate the gust.

THE CONTROL MODEL

For the control, we assume that a distributed torque actuator and sensors for measuring the response are embedded in the structure of the wing. We propose a linear constitutive relationship between the applied torque $\mathcal{T}(t)$ of the actuator and the input voltage $V(t)$ to the actuator:

$$\mathcal{T}(t) = K_0\, V(t) \tag{9}$$

To control the oscillations of the wing, we use a standard PID controller with the following control law:

$$V(t) = K_1 \dot{\alpha}(L,t) + K_2 \ddot{\alpha}(L,t) + K_3 \dot{w}(L,t) + K_4 \ddot{w}(L,t) \tag{10}$$

The gains K_1, K_2, K_3, and K_4 can be determined approximately using standard linear theory techniques, such as pole placement or loop shaping, and then fine tuned, if necessary.

COMBINING THE MODELS

A difficult, but essential task is to combine the structural, aerodynamic, and control models. This can be a challenge because the aerodynamic and structural problems are separate problems solved over mutually exclusive domains that share a common, time-varying boundary. It is where the two domains meet–on the wing surface–that all of the physics that make an aeroelastic problem interesting and challenging emerge.

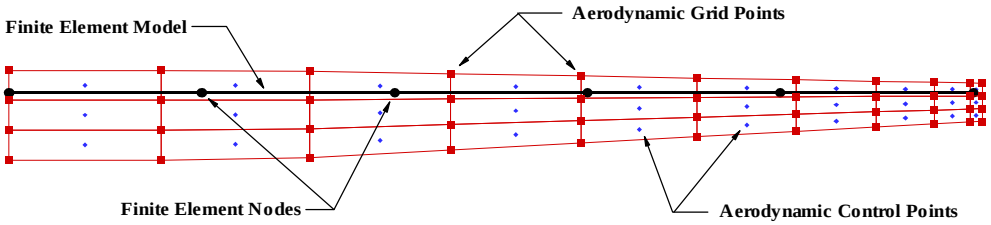

Figure 3: Simplified picture showing the overlay of the aerodynamic and structural grids.

Specifically, the three things that we must accomplish are 1) map the motions of the structural grid onto the aerodynamic grid, 2) map the aerodynamic loads onto the structural grid, and 3) map the control forces onto the structural grid.

In Figure 3 we show the superposition of sample aerodynamic and structural grids. The displacements of the points in the aerodynamic grid are calculated by assuming that they are attached to the elastic axis via a rigid link, which is perpendicular to the elastic axis. The displacement of the aerodynamic grid point $\mathbf{u}_A$ is approximated by the following linear relationship:

$$\mathbf{u}_A = G\mathbf{u}_S \tag{11}$$

where $\mathbf{u}_S$ is the vector of displacements and rotations of the elastic axis at the location of the "rigid link" and G is a constant matrix that is defined about the undeformed position of the wing.

The aerodynamic loads are transferred from the aerodynamic grid to the structural grid by assuming that the work done by the aerodynamic loads $\mathbf{F}_A^A$ during a virtual displacement of the aerodynamic grid $\delta\mathbf{u}_A$ is equal to the work done by the equivalent structural loads $\mathbf{F}_A^S$ during a virtual displacement of the structural grid $\delta\mathbf{u}_S$. The result is

$$\mathbf{F}_A^S = G^T\,\mathbf{F}_A^A \tag{12}$$

where G is the same matrix that relates the displacements of the grids and the superscript T indicates the transpose.

The control forces are defined over the original domain of the beam, before the discretization is performed. The finite-element nodal forces are found by projecting the distributed torque onto the finite-element model by following the same approach used to discretize the beam. The resulting nodal control forces are

$$\mathbf{F}_C(t) = \left\{ 0 \quad 0 \quad \frac{1}{2} \,|\, 0 \quad 0 \quad 1 \,|\, 0 \quad 0 \quad 1 \,|\, \cdots \,|\, 0 \quad 0 \quad 1 \,|\, 0 \quad 0 \quad \frac{1}{2} \right\}^T \mathcal{T}(t)$$

when the torque $\mathcal{T}(t)$ has no spatial dependence.

NUMERICAL SOLUTION

The solution is obtained by numerically integrating all of the governing equations simultaneously in the time domain. The procedure is based on Hamming's fourth-order predictor-corrector algorithm. We begin the calculations at each time step by convecting the wake. Then, using the current loads and velocities, we predict the solution of the equations governing the structure and use this solution to predict the positions and velocities of the aerodynamic grid points at the next time step. Using the latest predictions to obtain the boundary conditions for the aerodynamic model, we calculate aerodynamic loads at the new time step and use them in the structural model to correct the predicted positions and velocities. We repeat the last step until there is convergence; we do not re-calculate the wake during this iteration.

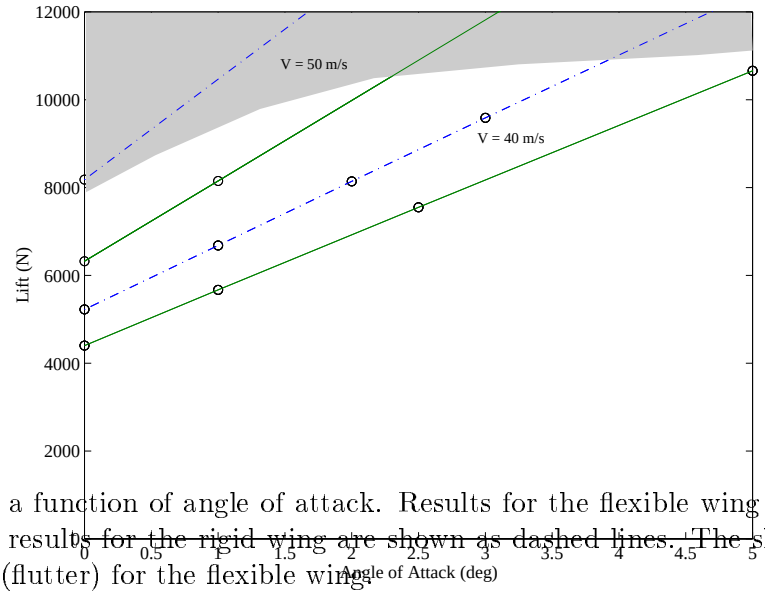

Figure 4: Lift force as a function of angle of attack. Results for the flexible wing are shown as solid lines and the corresponding results for the rigid wing are shown as dashed lines. The shaded area is the region of dynamic instability (flutter) for the flexible wing.

RESULTS

In this section, we briefly present some results of the simulations of the aeroelastic response of a typical HALE aircraft wing. We retain three modes for the structural dynamics, they correspond to the first bending mode, the first torsion mode, and the second bending mode of the uncoupled (i.e., $r_x = 0$) structural problem.

For this particular wing, the static response becomes unstable when the second (first torsion) and third (second bending) modes combine in a flutter response. In Figure 4 we show the flight envelope of the wing with the shaded area representing the regions of dynamic (flutter) responses. Also shown in the figure is the influence of the elasticity on the static aeroelastic response. If we ignore the flexibility of the wing, that is, assume that it is rigid, we obtain the dashed lines in Figure 4 whereas, if we consider the wing flexibility, we obtain the solid lines. The elastic effects greatly influence the response, not only introducing the possibility of flutter, but decreasing the net lift force (by as much as 20%) that the wing generates at any given speed and angle of attack.

In Figure 5a, we show a typical flutter response of the wing and in Figure 5b we show the application of the linear PID controller at time $t = 2500$ to a large and still growing flutter response. The controller quickly suppresses the flutter oscillations.

Figure 6 shows the envelope of the wing response at a stable flutter condition. As we can see more clearly in this figure, the wing is oscillating about its unstable equilibrium position, and it is apparent that, for this wing, we cannot accurately predict the response of the wing by assuming that it occurs near or around the zero deflection position.

Finally, we show the controlled response of the wing to a perturbation-type gust. The maximum gust velocity is approximately 15% of the freestream velocity and gust has frequency content near all three of the system mode frequencies. The control is the same as that used for the flutter suppression, but shows only marginal success in this test case.

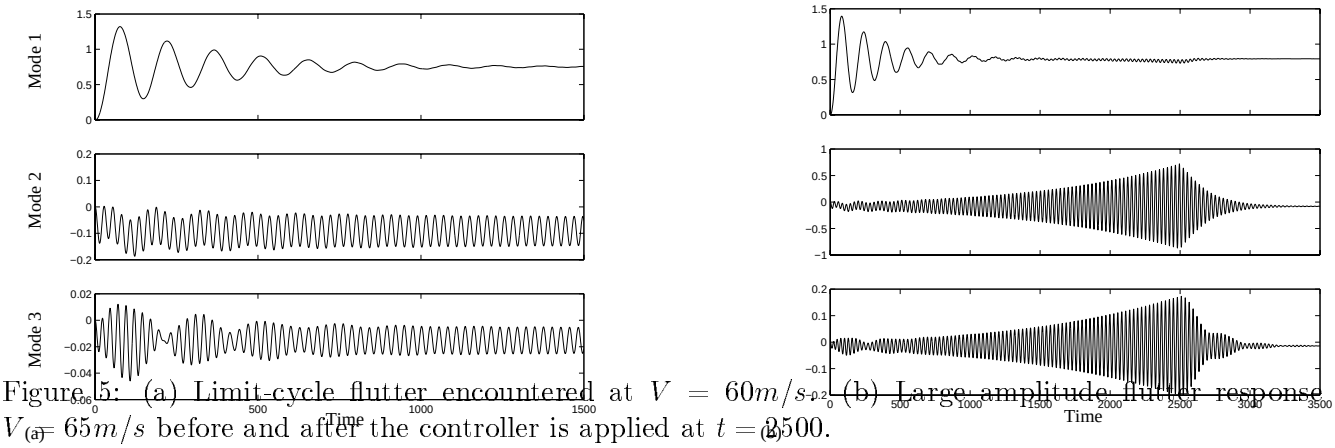

Figure 5: (a) Limit-cycle flutter encountered at $V = 60m/s$. (b) Large amplitude flutter response at $V = 65m/s$ before and after the controller is applied at $t = 2500$.

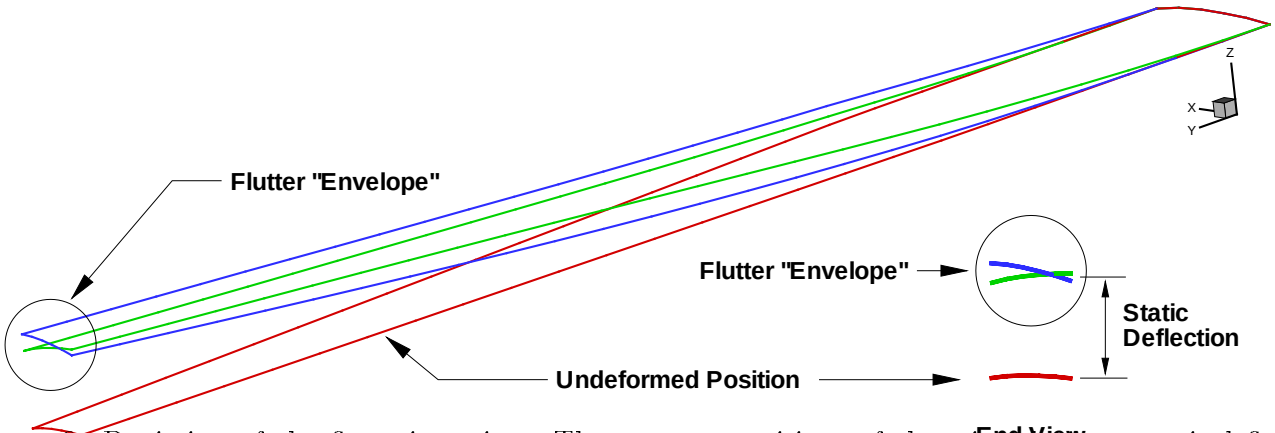

Figure 6: Depiction of the fluttering wing. The extreme positions of the wing during a typical flutter response are shown superimposed on the undeformed wing position.

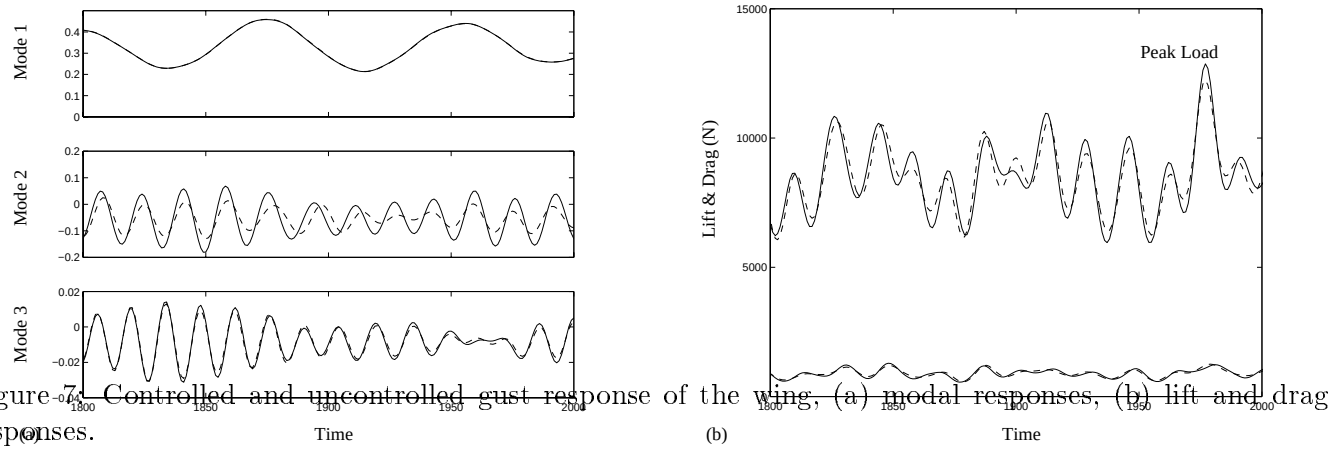

Figure 7. Controlled and uncontrolled gust response of the wing, (a) modal responses, (b) lift and drag responses.

CONCLUSIONS

In this paper, we have presented a method for predicting the response of dynamical systems in which the interaction between the fluid and structure parts is important. We have demonstrated the method using a smart HALE aircraft wing as an example and have described the flight envelope for the wing in terms of the lift force on, the angle of attack of, and the flight speed of the wing. We have performed simulations that show the dynamic response of the wing below, at, and above the critical flutter speed and that demonstrate the organization of the dynamic response as the flutter boundary is approached. Preliminary simulations of gust responses have also been performed via two different methods.

We have investigated several control strategies; the linear PID strategy was discussed herein and suppression of the flutter response above the flutter boundary was demonstrated. The same controller that readily suppresses the flutter oscillations of the wing was employed in a gust-load alleviation scheme with only marginal success. We are continuing work to optimize the controller to provide both significant gust-load alleviation as well as flutter suppression at much greater flight speeds.

Similar results have been obtained for investigations of the aeroelastic response a comparable wing, a business jet, and long span bridges. Work is also commencing in a parallel fashion to investigate the hydroelastic response of ships.

REFERENCES

[1] J. Luton and D. Mook, "Numerical simulations of flutter and its suppression by active control," *AIAA Journal* **31**(12), pp. 2312–2319, 1993.

[2] S. Preidikman and D. Mook, "A new method for actively suppressing flutter of suspension bridges," *Journal of Wind Engineering and Industrial Aerodynamics* **69–71**, pp. 955–974, 1997.

[3] S. Preidikman, *Numerical Simulations of Interactions Among Aerodynamics, Structural Dynamics, and Control Systems*. PhD thesis, Virginia Polytechnic Institute and State University, 1998.

[4] S. Preidikman and D. Mook, "Time-domain simulations of nonlinear, unsteady, aeroelastic behavior," in *MECOM99 Sexto Congreso Argentino De Mecanica Computacional*, (Mendoza, Argentina), September 6–10 1999.

[5] J. Cattarius, S. Preidikman, D. Mook, and D. Inman, "Vortex-lattice-method to analyze aerodynamic interference of wing/pylon/store configurations of an f16 wing," in *CEAS/AIAA/ICASE/NASA Langley International Forum on Aeroelasticity and Structural Dynamics*, (Williamsburg, VA), June 22-25 1999.

[6] D. Tang, E. Dowell, and K. Hall, "Limit cycle oscillations of a cantilevered wing in low subsonic flow," *AIAA Journal* **37**(3), pp. 364–371, 1999.

[7] S. Timoshenko, *Vibration Problems in Engineering*, McGraw Hill, 1974.

[8] R. Bisplinghoff, H. Ashley, and R. Halfman, *Aeroelasticity*, Dover Publications, Inc., Mineola, New York, 1996.

[9] Y. Fung, *An Introduction to the Theory of Aeroelasticity*, Dover Publications, Inc., New York, 1993.

[10] J. Rao, *Advanced Theory of Vibrations*, Wiley, New York, 1992.

[11] J. Reddy, *An Introduction to the Finite Element Method*, McGraw Hill, Boston, 1993.

[12] P. Konstadinopoulos, D. Thrasher, D. Mook, A. Nayfeh, and L. Watson, "Numerical model of unsteady subsonic aeroelastic behavior," *Journal of Aircraft* **22**, pp. 43–49, 1985.

[13] S. Belotserkovskii, *The Theory of Thin Wings in Subsonic Flow*, Plenum Press, New York, 1967.

[14] S. Belotserkovskii, "Study of the unsteady aerodynamics of lifting surfaces using the computer," *Annual Review of Fluid Mechanics* **9**, pp. 469–494, 1977.

[15] S. Belotserkovsky and I. Lifanov, *Method of Discrete Vortices*, CRC Press, Ann Arbor, 1993.

[16] R. Lewis, *Vortex Element Methods for Fluid Dynamic Analysis of Engineering Systems*, Cambridge University Press, Cambridge, 1991.

[17] J. Rom, B. Melamed, and D. Almosnino, "Experimental and nonlinear vortex lattice results for various wing-canard configurations," *Journal of Aircraft* **30**, pp. 207–212, 1993.

[18] J. Elzebda, D. Mook, and A. Nayfeh, "Numerical simulation of steady and unsteady, vorticity-dominated aerodynamic interference," *Journal of Aircraft* **31**, pp. 1031–1036, 1994.

[19] T. Sarpkaya, "Computational methods with vortices—the 1988 Freemen scholar lecture," *Journal of Fluids Engineering* **111**(75), pp. 5–52, 1989.

[20] M. Dornheim, "AeroVironment pushes limits of solar flight," *Aviation Week & Space Technology* **148**, pp. 54–57, 1998.

[21] F. Hoblit, *Gust Loads on Aircraft: Concepts and Applications*, AIAA Press, Washington, DC, 1988.